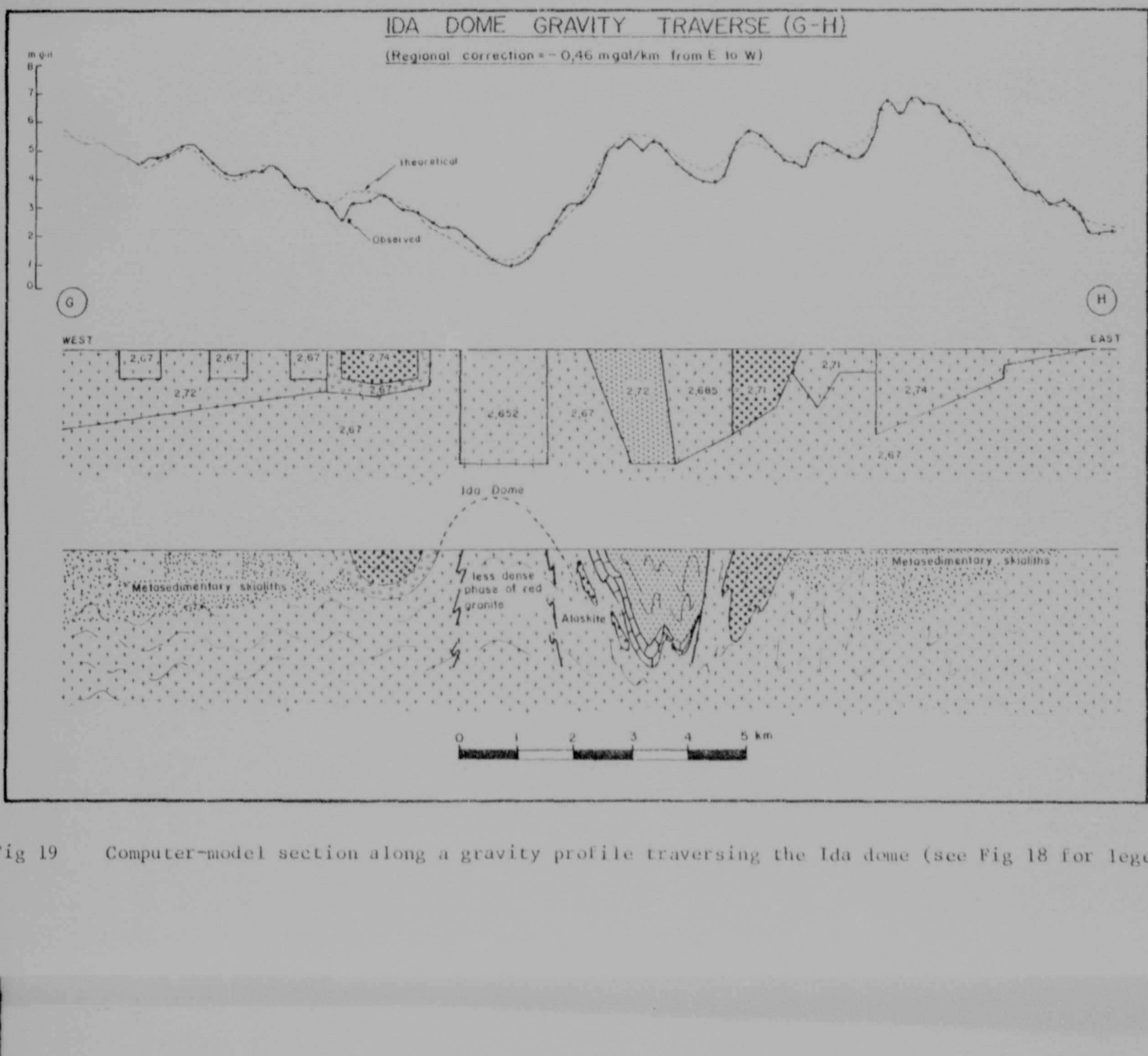

Fig 19 Computer-model section along a gravity profile traversing the Ida dome (see Fig 18 for legend)

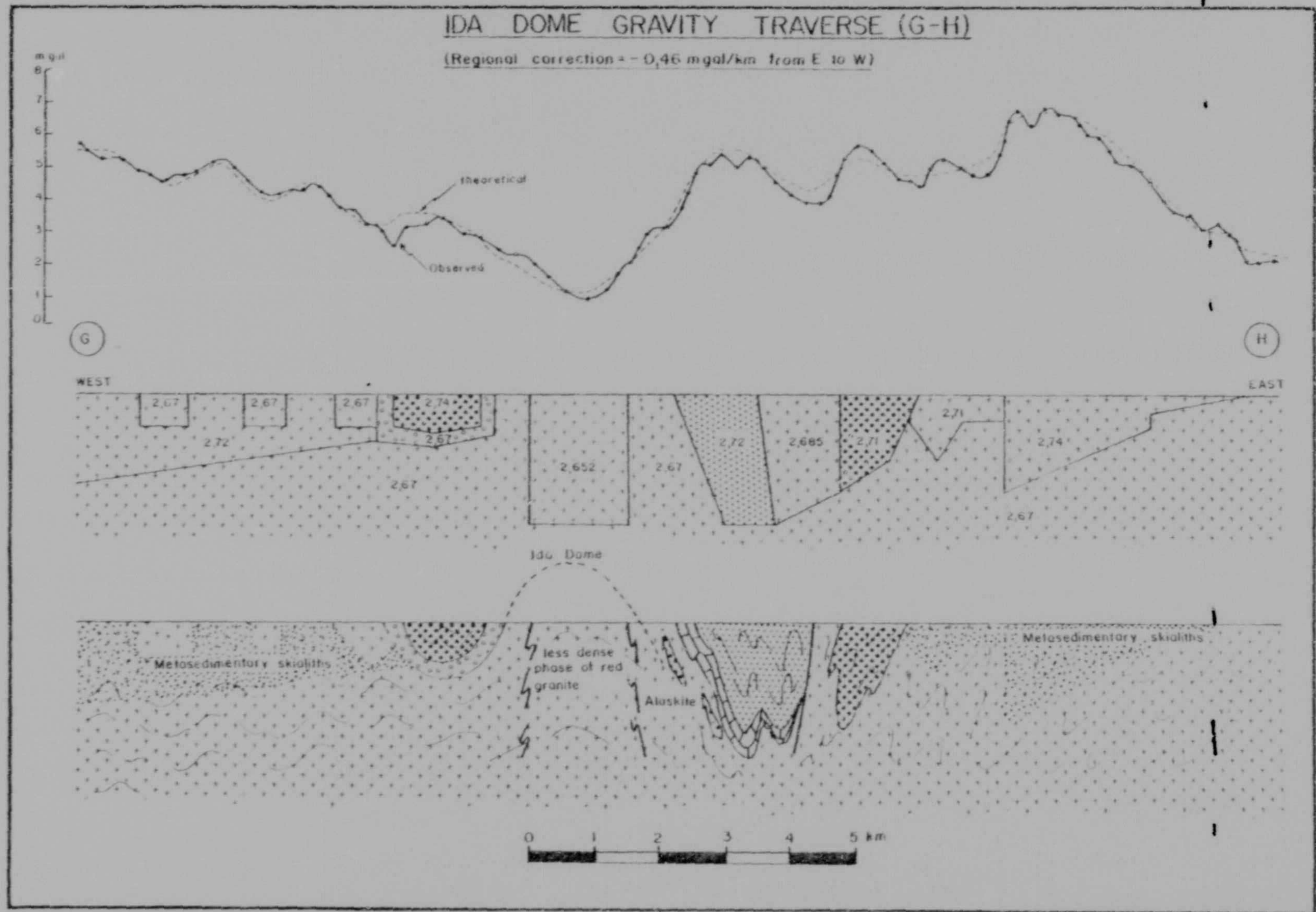

Fig 19 Computer-model section along a gravity profile traversing the Ida dome (see Fig 18 for legend)

putation of its gravitational field using the computer program of Talwani et al., (1959). The resultant theoretically calculated profile was compared to the observed profile for each of the traverses, and changes were made to the models (within the constraints of the known densities and geology) until a good agreement was found between the two profiles. Six computer runs were needed for each section, on average, to yield the block-models and best-fits shown in Figs 18 and 19.

Since the program calculates the gravity field of two-dimensional bodies only, two dimensionality had to be assumed for the dome structures traversed. Grant and West (1965) have described the criteria necessary for two dimensionality from which it is clear that elongate bodies, roughly 5 times longer than they are wide, may be considered to be two dimensional. The Ida and Rössing domes are only elongate by a factor of roughly 2,5 and the Tsaun dome is roughly circular making this assumption not entirely valid. This would not affect the model greatly, however, since it would result in a change either in the depth of burial of a particular non two-dimensional body, or its density contrast. In the latter respect the density contrast would in fact be slightly more than that given in the model sections. Nevertheless, in view of the approximate two dimensionality of the Rössing and Ida domes it is felt that the simplistic models calculated are, as a first approximation, realistic.

6.4 Discussion and Conclusions

The three model sections indicate the following:

i) Gravity lows are associated with the cores of the dome structures. These are of small amplitude and variable, being largest for the Ida dome as a result of the large mass of low density (Table VII) alaskitic granite that was traversed, and smallest for the Tsaun traverse along which the geology comprised, virtually exclusively, a series of Khan paragneisses. Other lows included that over basement, exposed in another dome on the Rössing traverse, and that southeast of the Tsaun dome, with which no particular structure is associated. The gravity lows are thus not pertinently related to the dome cores.

ii) The observed gravity anomalies can be explained entirely by near-surface changes in lithology. The gravity lows bear evidence for density heterogeneity, and hence gravitational instability must have prevailed at the time of dome formation causing diapiric ascent.

iii) The density contrasts yielding the best fits are small, never exceeding 0,10 $g.cm^{-3}$ and averaging 0,065 $g.cm^{-3}$, but nevertheless within the limits of the measured densities in Table VII. The models were only taken down to depths of 3 km since it was evident that any deeper bodies having the above density contrasts would not be readily evident on surface, particularly with the masking effect of the larger amplitude near surface anomalies. If the modelled bodies were, however, extended to greater depths, the given density contrasts would have to be reduced slightly to yield similar theoretical profiles.

In view of the above, particularly the small density contrasts, the author considers it unlikely that the gravitational instability would have been great enough in a viscous, rather than fluid, medium to be entirely responsible for dome formation. Heterogeneities acting as dome initiators would be essential and it could thus justifiably be argued that initial stocks of mobilised alaskite could have provided the necessary initiation for dome formation. The volume of this material as seen today in the domes is however small in relation to the size of the structures. Much of the lighter (and heavier) material could of course have been removed by erosion.

The key to the type of initiator required for many of the domes, however, lies in the non-random orientation of these structures. The orientations of the major axes of the Rössing, Ida, Goanikontes and Sandwich Bay domes are so similar, i.e. north-northeast, corresponding to the direction of the Welwitschia lineament zone (F4 structural episode), that an interplay with lateral stress fields must be called upon to explain their formation. These stresses need not necessarily have two initial-direction components, as is classically proposed to cause interference fold patterns. A uniform single direction of lateral stress acting on a series of laterally discontinuous formations (the Nosib depositories are excellent examples) would result in secondary stress fields of variable direction which, acting in harmony with gravitational components, could provide the necessary initiation for the dome structures. Whether these structures have a preferred orientation or not would depend on the strength of the initial field in relation to the secondary stress field/s generated by lateral lithological discontinuities.

The concept of gravitational instability between rocks of lower density (granites, gneisses and the Etusis Formation) and cover rocks of higher density (Khan Formation and carbonate rich rocks of the Swakop Group) cannot therefore be exclusively called upon as an explanation for the origin of the domes, although it undoubtedly played a major role. It is concluded that the attainment of gravitational (vertical) equilibrium in an environment of contrasting densities must have been controlled to a certain extent by the prominent lateral stress field/s prevailing at the time, i.e. the domes result from an interplay of both these components.

7 SUMMARY OF CONCLUSIONS

Qualitative and quantitative interpretation of the aeromagnetic data covering the western portion of the Damara orogenic belt, with special reference to the occurrence of uraniferous alaskitic granite and to the regional structure of the area, has revealed that:

i) All currently known uraniferous alaskitic granite occurrences of economic interest are associated, on a semi-regional basis, with prominent negative magnetic anomalies. The relationship is a stratigraphic one since the palaeomagnetic studies have shown that these negative anomalies arise from a pervasive remagnetisation of the Damaran rocks during the 500 Ma tectono-thermal event, with the retention thereof in rocks chiefly of the Khan Formation - a stratigraphic level with which the uraniferous granites are closely associated.

The higher and lower stratigraphic levels, viz. the Swakop Group, the late- to post-tectonic granites (e.g. Salem, Donkerhuk), the red granites and reactivated basement, have mostly either lost this direction, acquired a reversed 500 Ma direction, or attained a hybrid direction as a result of a later secondary magnetisation, possibly associated with the period of late- to post-Karoo igneous intrusion. No abnormal negative magnetic anomaly thus arises from rocks of the Swakop Group and associated granites. Induced or secondary magnetisation has resulted in either undisturbed fields or positive magnetic anomalies over these rocks.

The effect of the retention of the 500 Ma thermo-remanent direction in the Khan Formation is that areas of outcrop or of shallow suboutcrop of these rocks, as occur in anticlinal and dome structures, are hallmarked by negative anomalies. The stratigraphic relationship with the uraniferous granite occurrences thus constitutes an important prospecting criterion. The fact that the negative anomalies may be used as a Group stratigraphic marker also has important mapping implications since suboutcrops of the Khan formation may be identified in areas covered by aeolian sand, scree and duricrust deposits. On this basis, suboutcrops of these rocks have been outlined south of the Kuiseb River and a prominent dome structure east of Sandwich Bay has been identified.

ii) The virtual geomagnetic pole (VGP) position derived for the Damara orogeny, which plots on the Moroccan coast, is in good agreement with other pole positions for that period. The VGP for the basement rocks suggests that a slight change may need to be made to the polar wander path of McElhinny and McWilliams (1977) to accommodate it. On this assumption the polar-wander path implies an age for the basement rocks of approximately 2 150 Ma. This is within the limits of accuracy of a radiometric U-Pb age of 1 925 Ma (+330, -280 Ma) determined by Jacob et al., (1978) for these rocks.

iii) Regarding the phenomenon of the so-called oxidation haloes, it is concluded from the palaeomagnetic results that the uraniferous alaskitic granite, enclosed by the haloes, is the original fresh rock and that the haloes themselves represent an encroaching alteration front (through oxidation) which has already destroyed the initial thermo-remanent magnetisation of the surrounding rock.

iv) A TiO_2-FeO-Fe_2O_3 ternary composition diagram for the rocks sampled shows that more than one magnetic-mineral phase is present, viz. certain samples follow the titanomagnetite solid solution series whereas the majority follow the hematite-ilmenite series. It is concluded that the latter may have an important bearing on the observed reversed directions of magnetisation, suggesting self reversal at possibly two sites.

v) A number of structural lineaments and broader lineament zones are immediately evident from the aeromagnetic data which, apart from the Okahandja lineament, are recognised and named for the the first time in this text. They include:

- the Uis lineament zone
- the Omaruru lineament
- the Welwitschia lineament zone and the less prominent
- Wlotzka and Abbabis lineament zones.

Computer modelling studies support the hypothesis that these magnetic lineament zones are in fact areas of uplift or geanticlinal ridges bounded by relatively rapid monoclinal downfolding of the stratigraphy. The most severe downfolding and change in structural style occurs across the Okahandja lineament. The modelling studies support the conclusions of Miller (1979) that uplift along the northern margin of this lineament was very large, possibly of the order of 20 km. The nature of the geanticlinal ridging would appear, from the magnetic gradients and anomaly amplitudes, to be fault controlled.

A consideration of the geodynamic models proposed for the belt north of the southern zone, i.e. a plate-tectonic model (by plate collision - Burke and Dewey, 1972 and 1973; and Burke et al., 1977) as opposed to the ensialic, modified multiple-aulacogen model of Martin and Porada (1977), has shown a strong compatibility between computer modelling results and the latter model. It is thus concluded that the magnetic lineament zones represent initial fault-bounded depositories, for the clastic Nosib sediments, which have subsequently been buoyed up by varying degrees, as a result of gravitational instability, to form the geanticlinal ridges which they represent today.

vi) The identification of the north-northeasterly trending Welwitschia lineament zone has revealed that a post-F3 (northeast) structural phase, F4, oriented north-northeast is of particular significance to the emplacement of uraniferous granite since, firstly, the major fold axes of the domes and structures with which these occurrences are associated have this orientation and, secondly, the currently known occurrences are situated along the Welwitschia lineament zone. The latter relationship is also in part probably due to the fact that the lower stratigraphic levels, with which these occurrences are mostly associated, are exposed along this geanticlinal ridge.

In view of the above relationships it is likely that the F4 structural episode is of the same age as the associated alaskitic granites, i.e. 470 Ma.

vii) On the basis of the above conclusions (i and vi) it is possible that the dome structure, identified magnetically east of Sandwich Bay, may provide the correct structural and stratigraphic setting for the location of another Rössing-type uranium deposit.

viii) A close correlation exists between positive magnetic anomalies and high radiometric responses over the red granites, reactivated basement and, to a lesser extent, the Salem Granite Suite and other late- to post-tectonic granites. In the former two cases the high radiometric responses are due to raised concentrations of thorium coupled with sporadic but non-economic increases in the concentration of uranium. In the latter cases these responses are due mostly to raised thorium concentrations. A direction of magnetisation hybrid between the 500 Ma tectonothermal direction and a later or present-day direction, and/or a reversed 500 Ma direction, are responsible for the associated positive magnetic anomalies in the various rock types.

The magnetic/radiometric relationship over the late- to post-tectonic granites immediately south of the Brandberg-Cape Cross line indicates that these rocks may be of a different genetic origin to the Donkerhuk granite and to the Salem granite outcrops in the south and east of the area.

In view of the raised levels of radioactivity over most of the granites and gneisses in the area, the total-count radiometric data is of little value as an aid to mapping. Spectrometric surveys would, however, be of value in mapping the increases in potassium concentration in the late-phase alaskitic granite differentiates, with which the uranium occurrences are associated.

ix) Quantitative interpretation of gravity traverses, conducted over three dome structures with which uranium occurrences are associated, has shown that although gravity lows are associated (non-uniquely, however) with the core of the domes, these are minor and are entirely explained by small density contrasts resulting from near-surface variations in lithology. Gravitational instability between rocks of lower density (granites, gneisses and the Etusis Formation) and cover rocks of higher density (Khan Formation and carbonate rich rocks of the Swakop Group) thus undoubtedly prevailed at the time of dome formation but cannot be called upon exclusively as an explanation for the origin of the domes. Lateral stress is proposed as the dome initiator in a gravitationally unstable environment, particularly in view of the non-random orientation (north-northeast, F4) of the major axes of, for example, the Rössing, Ida, Goanikontes and Sandwich Bay domes. It is thus concluded that the attainment of gravitational (vertical) equilibrium in an environment of contrasting densities must have been controlled to a certain extent by the prominent lateral stress fields prevailing at the time, i.e. the domes result from an interplay of both these components.

8 APPENDIX

APPENDIX A1.

TABLE A1. : LOCALITIES, LITHOLOGIES AND LOCAL GEOMAGNETIC FIELD INTENSITY OF THE PALAEOMAGNETIC SAMPLES SITES

Site Number	SITE LOCALITIES			Geomagnetic intensity Total field (nT) *	Formational unit, Lithology
	Approximate Locality	Latitude	Longitude		
1	Rössing mine	22°28,48'	15°2,79'	30 230 (low)	Alaskitic granite
2	Rössing mine	22°28,48'	15°2,79'	30 950 (high)	Khan Formation
3	Rössing mountain	22°30,44'	14°51,58'	29 790 (low)	Khan Formation
4	Rössing dome	22°27,49'	15°3,66'	29 820 (low)	Red granite
5	Rössing dome	22°26,66'	15°3,48'	31 220 (high)	Red granite
6	Farm Valancia (122)	22°20,91'	15°13,54'	30 850 (normal)	Alaskitic granite
7	Farm Valencia (122)	22°19,15'	15°14,63'	30 325 (low)	Etusis Formation
8	Farm Valencia (122)	22°19,15'	15°14,16'	30 540 (low)	Etusis Formation
9	Farm Valencia (122)	22°19,01'	15°14,85'	30 020 (low)	Etusis Formation
10	Farm Palmenhorst (38)	22°40,82'	14°51,21'	30 300 (low)	Khan Formation
11	Farm Palmenhorst (38)	22°40,95'	14°51,03'	30 580 (low)	Alaskitic granite
12	Farm Palmenhorst (38)	22°40,90'	14°51,21'	30 080 (low)	Red granite
13	Trekkopje Siding	22°17,07'	15°6,37'	31 090 (high)	Etusis Formation
14	Trekkopje Siding	21°17,04'	15°6,26'	30 990 (high)	Alaskitic granite
15	Trekkopje Siding	22°17,04'	15°6,26'	31 350 (high)	Red granite
16	Mile 72	21°50,77'	14°11,14'	30 770 (normal)	Salem granite
17	Tsaun beacon	21°40,1'	14°33,9'	30 550 (low)	Alaskitic granite
18	Tsaun beacon	21°39,9'	14°33,5'	30 600 (low)	Khan Formation
19	Tsaun beacon	21°39,9'	14°33,5'	30 600 (low)	Khan Formation
20	Kuiseb River	23°20,73'	14°50,66'	30 550 (low)	Basement granite-gneiss
21	Kuiseb River	23°14,86'	14°55,37'	30 575 (low)	Basement granite-gneiss
22	Hollands dome	22°46,04'	15°1,06'	30 140 (low)	Alaskite granite
23	Hollands dome	22°45,86'	15°1,12'	30 420 (low)	Khan Formation
24	Hollands dome	22°45,86'	15°1,12'	30 420 (low)	Alaskitic granite
25	Ida mine	22°41,68'	15°1,64'	29 800 (low)	Khan Formation
26	Ida mine	22°41,68'	15°1,64'	29 850 (low)	Alaskitic granite
27	Ida mine	22°41,68'	15°1,82'	30 560 (low)	Alaskitic granite
28	Hollands dome	22°45,86'	15°0,94'	31 400 (high)	Red granite
29	Ida dome	22°45,24'	15°0,29'	30 705 (normal)	Alaskitic granite
30	Farm Onanis (121)	22°51,81'	15°43,68'	30 590 (low)	Donkerhuk Granite
31	Farm Onanis (121)	22°49,16'	15°44,63'	30 600 (low)	Donkerhuk Granite
32	Farm Solitaire	23°56,40'	15°52,20'	30 205 (low)	Piksteel Granodiorite
33	Farm 399 (Saagberg ?)	23°43,20'	15°52,80'	30 200 (low)	Piksteel Granodiorite
34	Farm Abbabis (70)	22°10,20'	15°40,80'	30 850 (normal)	Basement granite-gneiss
35	Farm Ubib-W (76)	22°10,80'	15°33,60'	31 000 (high)	Abbabis Met. Complex
36	Farm Ubib-W (76)	22°10,80'	15°33,00'	31 000 (high)	Abbabis Met. Complex
37	Cape Cross	21°48,00'	14°1,80'	31 300 (high)	Basalt
38	Cape Cross	21°46,80'	14°00,60'	31 400 (high)	Basalt
39	Tsaun beacon	21°35,40'	14°33,00'	30 600 (low)	Khan Formation
40	Tsaun beacon	21°34,80'	14°31,20'	30 600 (low)	Khan Formation
41	Tsaun beacon	21°35,40'	14°27,00'	30 800 (normal)	Khan Formation
42	Brandberg	21°7,20'	14°38,40'	31 250 (high)	Granite
43	Brandberg	21°6,00'	14°38,40'	31 300 (high)	Granite
44	Farm Anibib (136)	21°30,60'	15°33,00'	31 150 (high)	Erongo granite
45	Farm Ameib (60)	21°45,60'	15°36,60'	31 300 (high)	Erongo granite
46	Wlotska's Baken	22°21,60'	14°28,20'	30 480 (low)	Khan Formation
47	Farm Goanikontes (28)	22°38,40'	14°46,80'	31 170 (high)	Swakop Group
48	Swakopmund (Vineta)	22°39,00'	14°31,80'	31 000 (high)	Red granite

* Determined at the time of sampling using a Geometrics Proton Precession Magnetometer. The value given is the average of five readings taken at each site, viz. at the site and approximately 50 m north, south, east and west of it.

APPENDIX A2.

Stereographic Plots of the NRM and AF-Demagnetised Directions of Sites 1 - 48.

(Note: the demagnetising field given for each site is that applied to the core specimens which gave the grouping shown in the right-hand stereographic plot.)

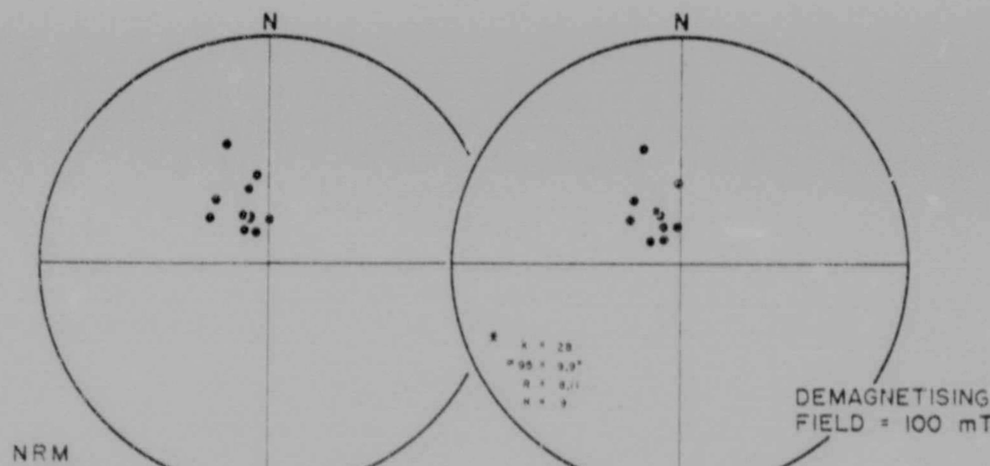

SITE 1 RÖSSING MINE : ALASKITIC GRANITE

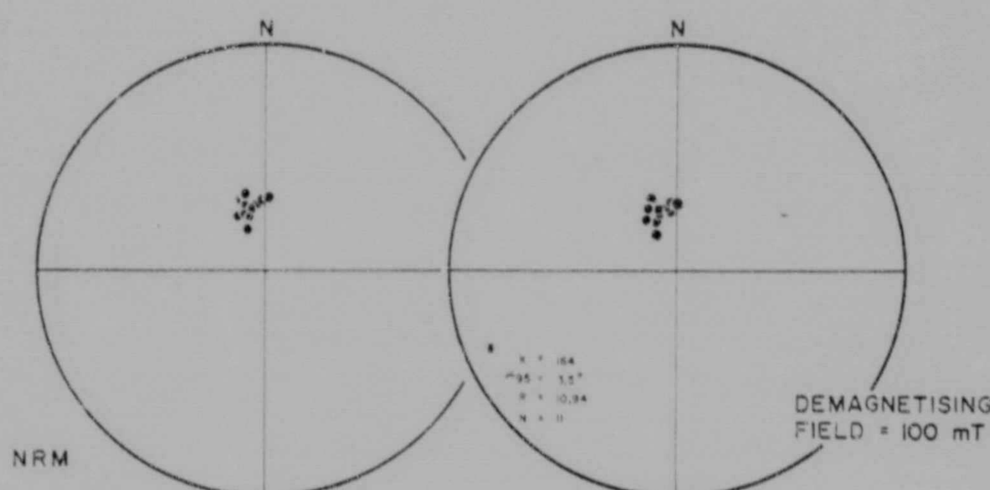

SITE 2 RÖSSING MINE : KHAN FORMATION

SITE 3 RÖSSING MOUNTAIN : KHAN FORMATION

- • POSITIVE INCLINATION
- ○ NEGATIVE INCLINATION
- ■,□ SITE MEANS
- * FISHER STATISTICS AS DEFINED IN TEXT

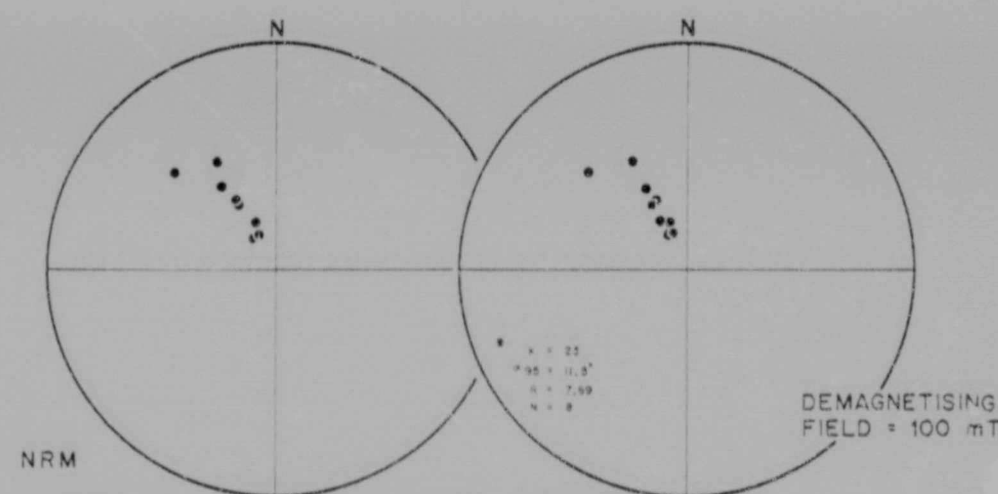

SITE 4 ROSSING DOME : RED GRANITE

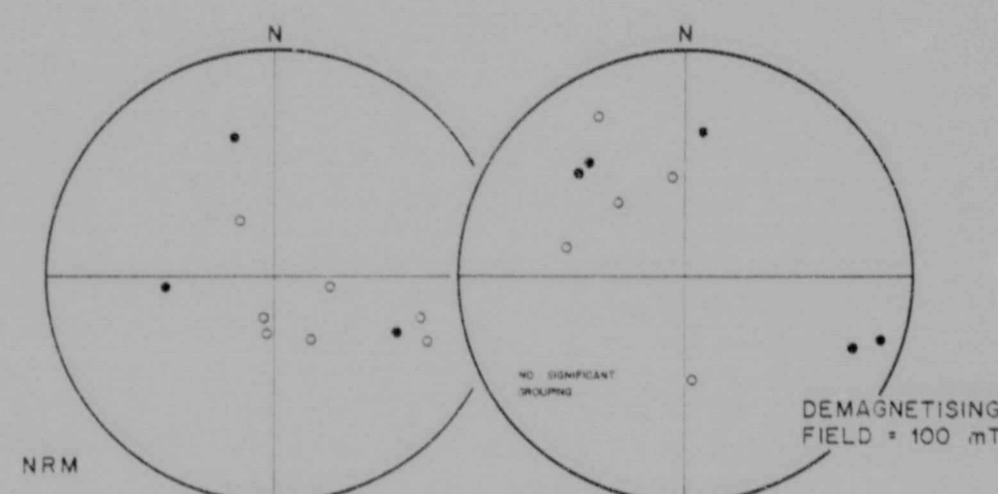

SITE 5 ROSSING DOME : RED GRANITE

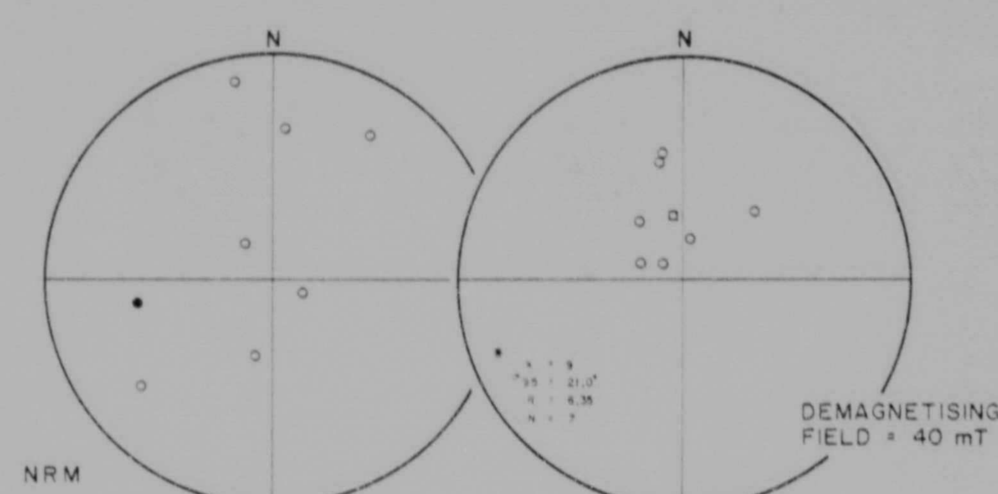

SITE 6 VALENCIA : ALASKITIC GRANITE

• POSITIVE INCLINATION ■ □ SITE MEANS

○ NEGATIVE INCLINATION • FISHER STATISTICS AS DEFINED IN TEXT

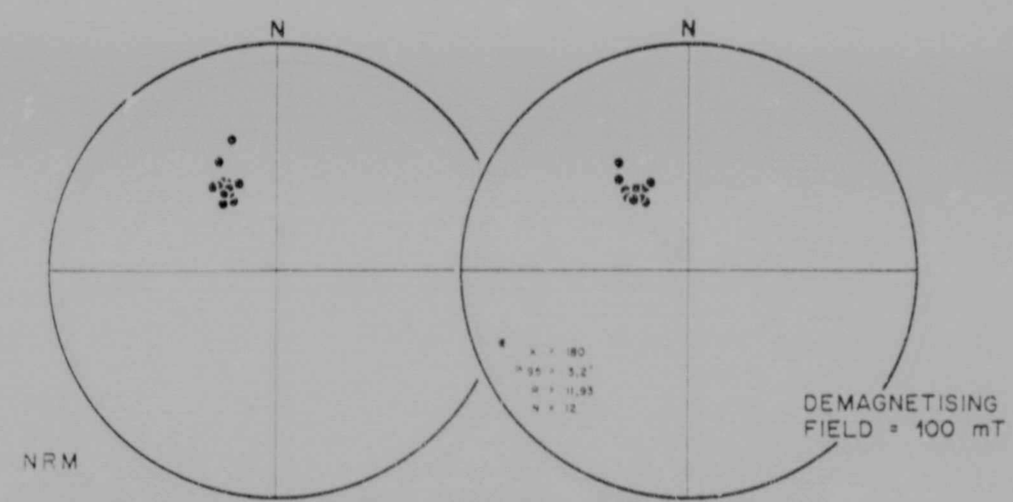

SITE 7 VALENCIA : ETUSIS FORMATION

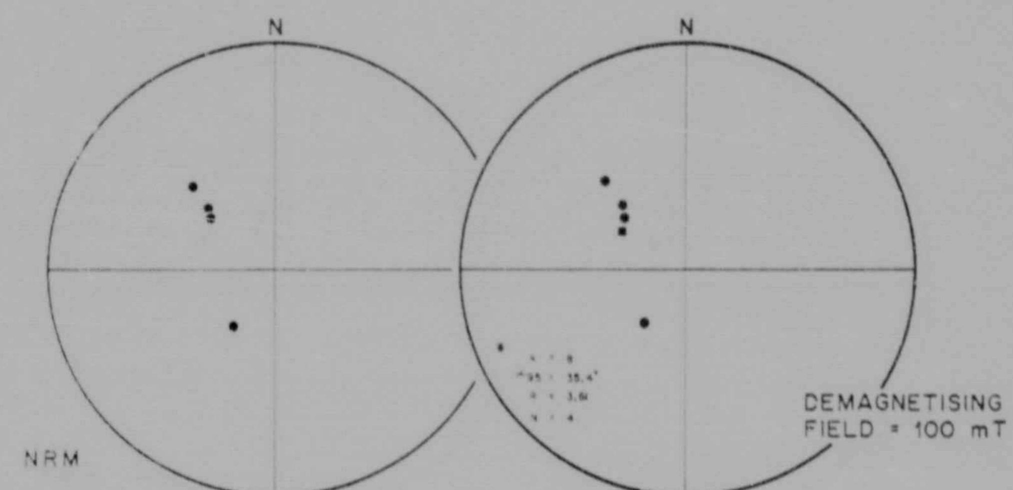

SITE 8 VALENCIA : ETUSIS FORMATION

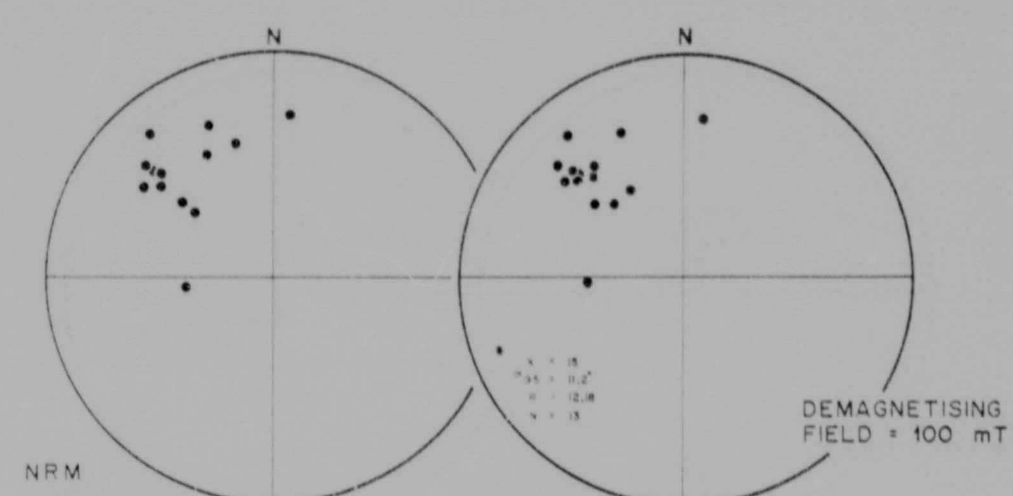

SITE 9 VALENCIA : ETUSIS FORMATION

● POSITIVE INCLINATION ■ □ SITE MEANS

○ NEGATIVE INCLINATION • FISHER STATISTICS AS DEFINED IN TEXT

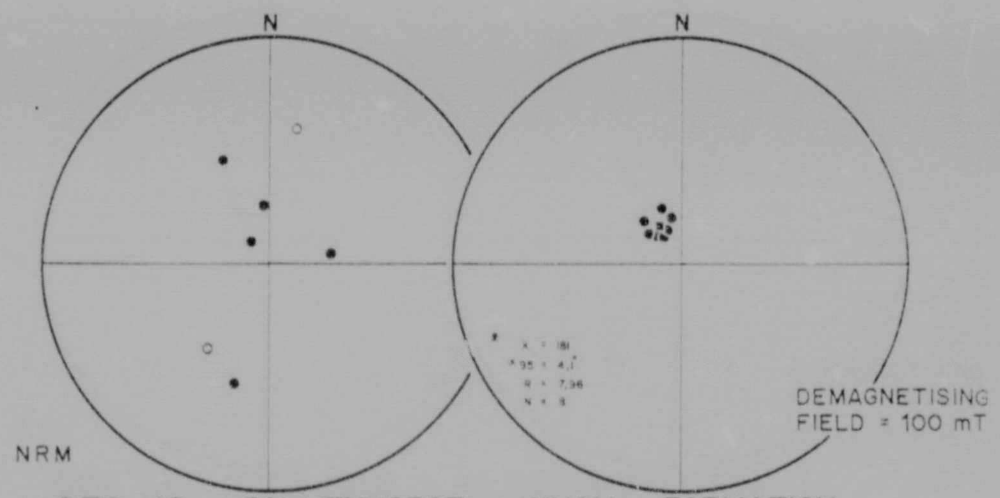

SITE 10 PALMENHORST : KHAN FORMATION

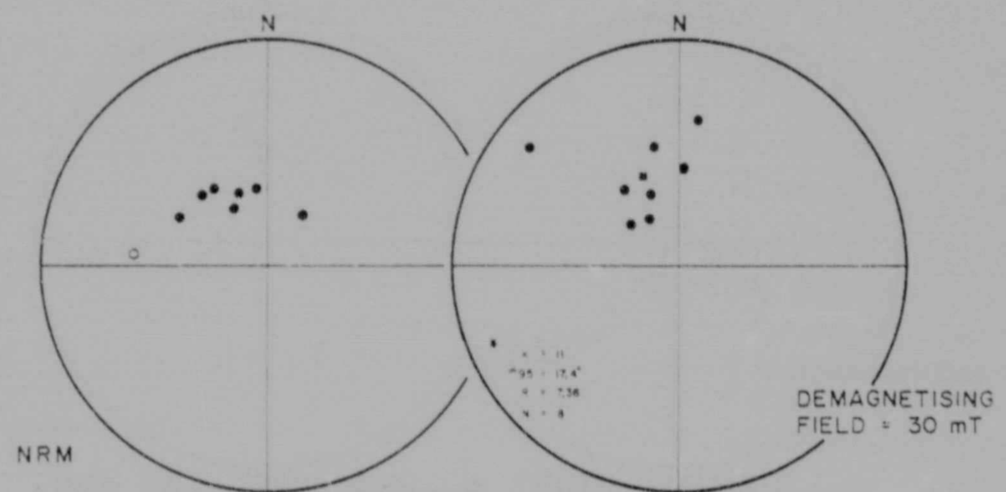

SITE 11 PALMENHORST : ALASKITIC GRANITE

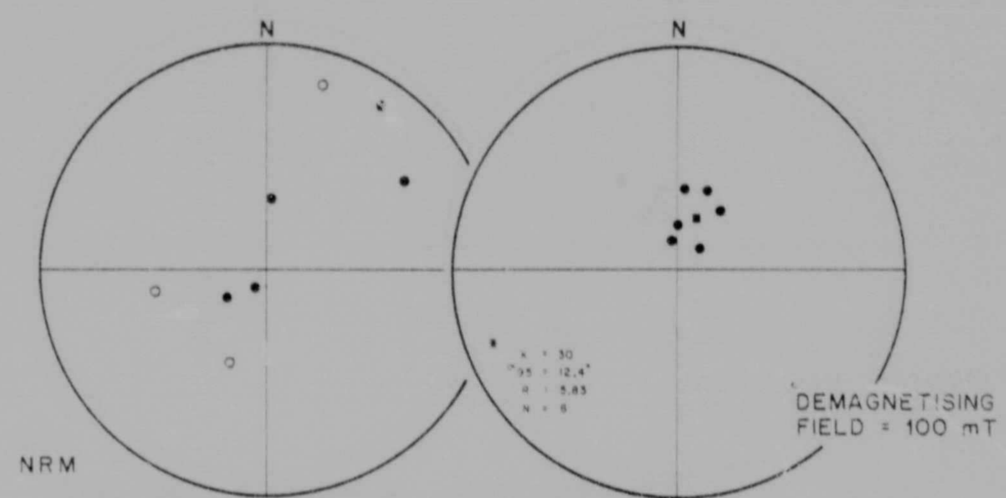

SITE 12 PALMENHORST : RED GRANITE

• POSITIVE INCLINATION ▪ ▫ SITE MEANS

○ NEGATIVE INCLINATION • FISHER STATISTICS AS DEFINED IN TEXT

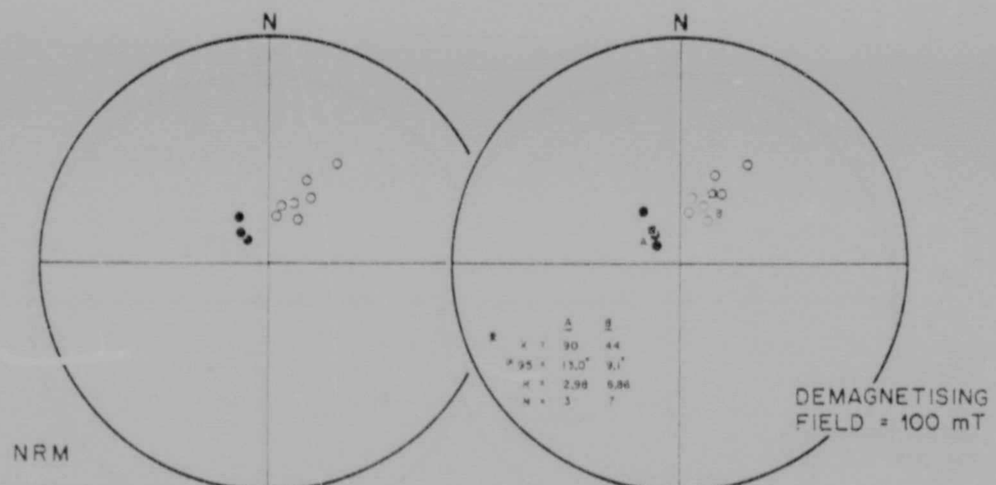

SITE 13 TREKKOPJE : KHAN FORMATION

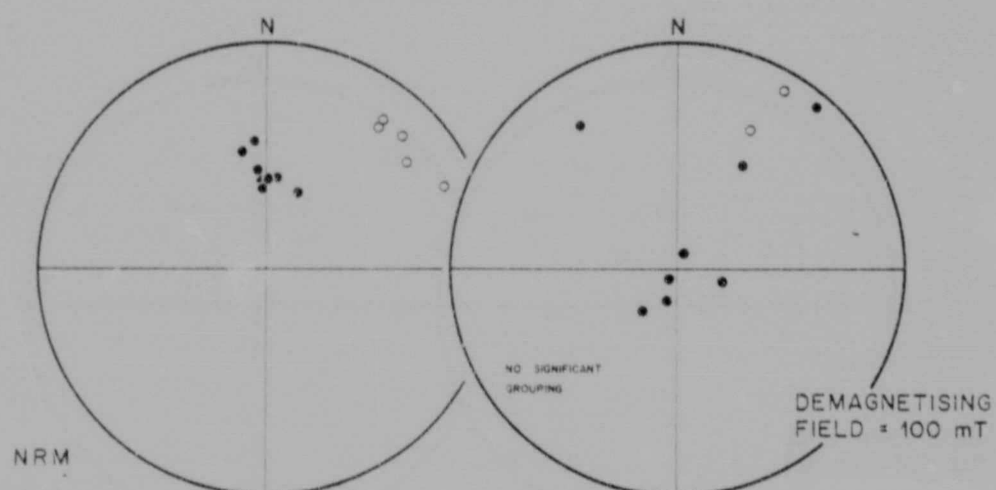

SITE 14 TREKKOPJE : ALASKITIC GRANITE

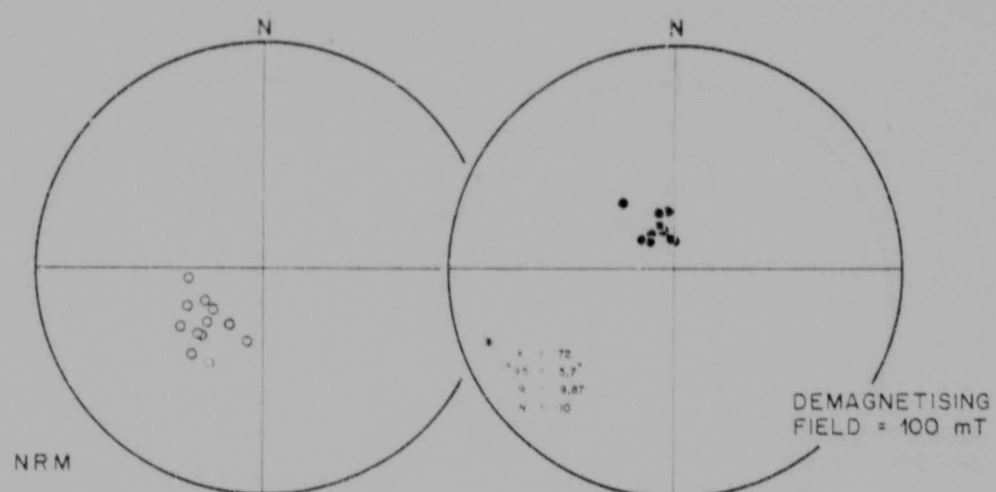

SITE 15 TREKKOPJE : RED GRANITE

● POSITIVE INCLINATION
○ NEGATIVE INCLINATION
■ □ SITE MEANS
* FISHER STATISTICS AS DEFINED IN TEXT

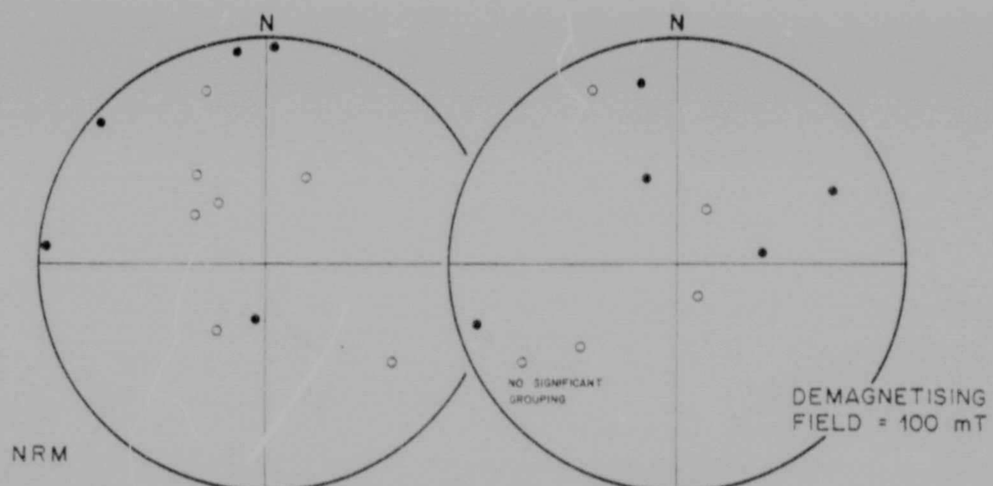

SITE 16 MILE 72 : SALEM GRANITE

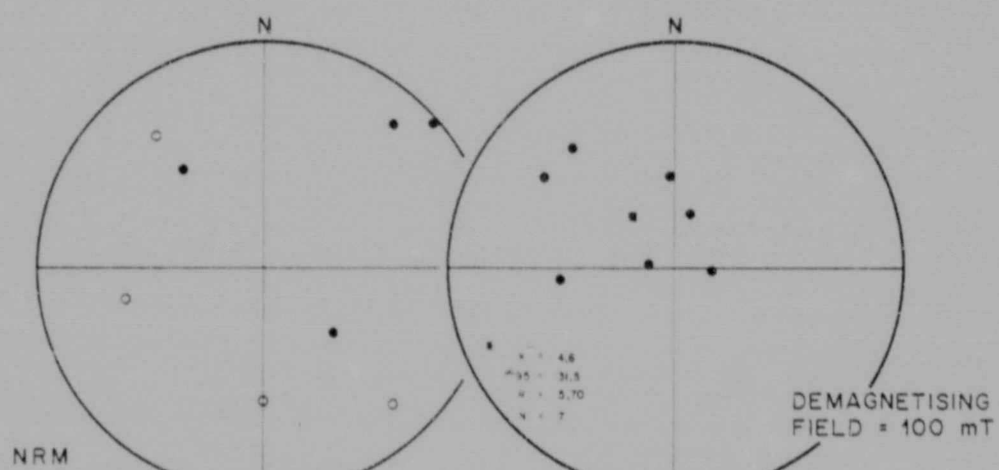

SITE 17 TSAUN BEACON : ALASKITIC GRANITE

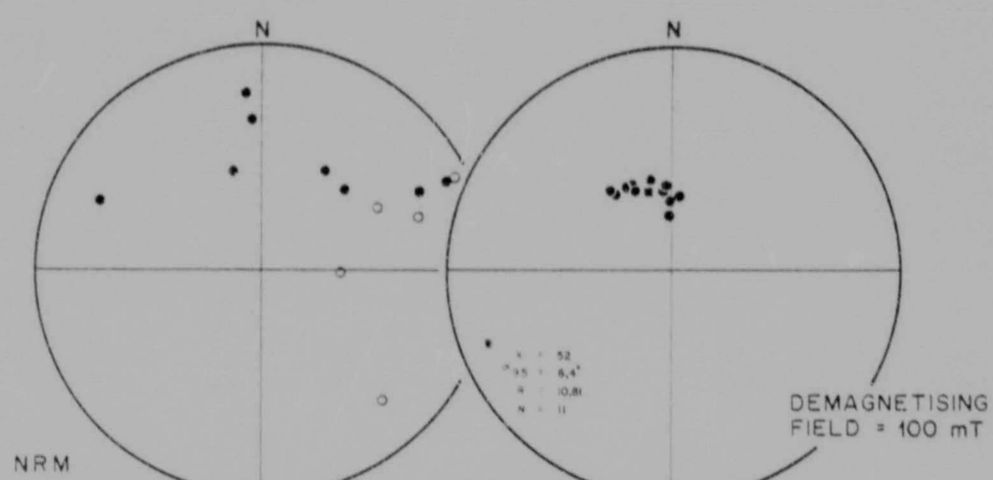

SITE 18 TSAUN BEACON : KHAN FORMATION

• POSITIVE INCLINATION

○ NEGATIVE INCLINATION

■,□ SITE MEANS

* FISHER STATISTICS AS DEFINED IN TEXT

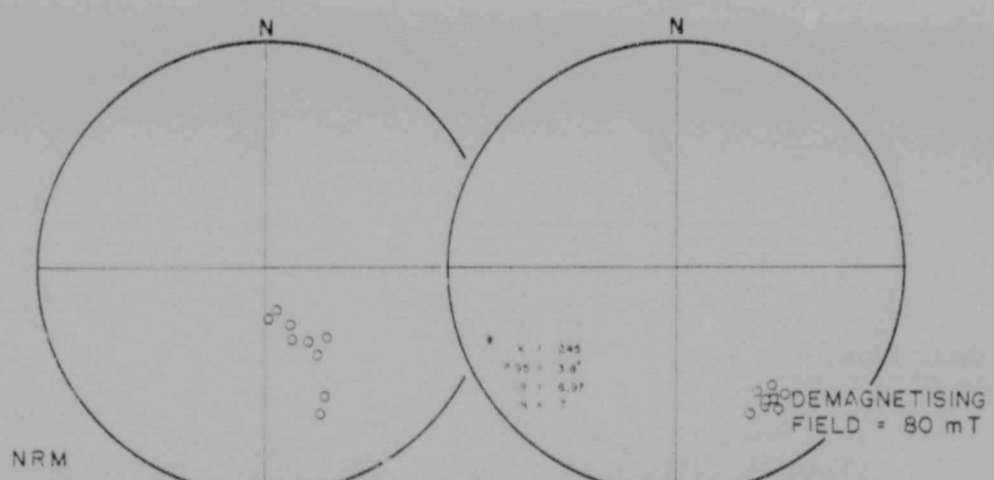

SITE 19 TSAUN BEACON : KHAN FORMATION

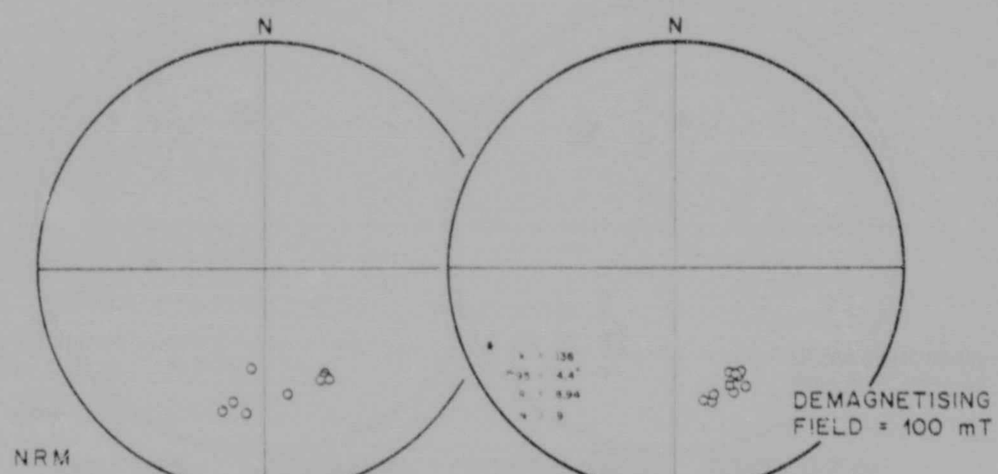

SITE 20 KUISEB RIVER : BASEMENT GRANITE - GNEISS

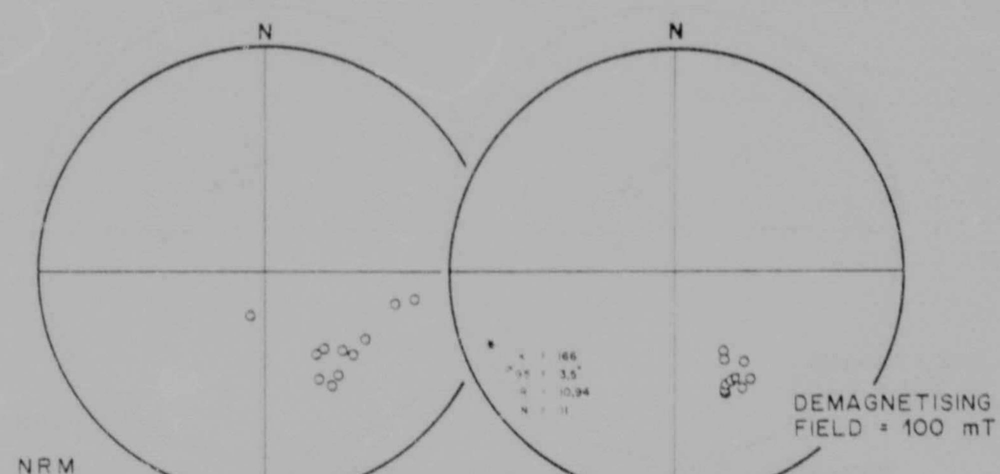

SITE 21 KUISEB RIVER : BASEMENT GRANITE - GNEISS

• POSITIVE INCLINATION ■□ SITE MEANS

○ NEGATIVE INCLINATION • FISHER STATISTICS AS DEFINED IN TEXT

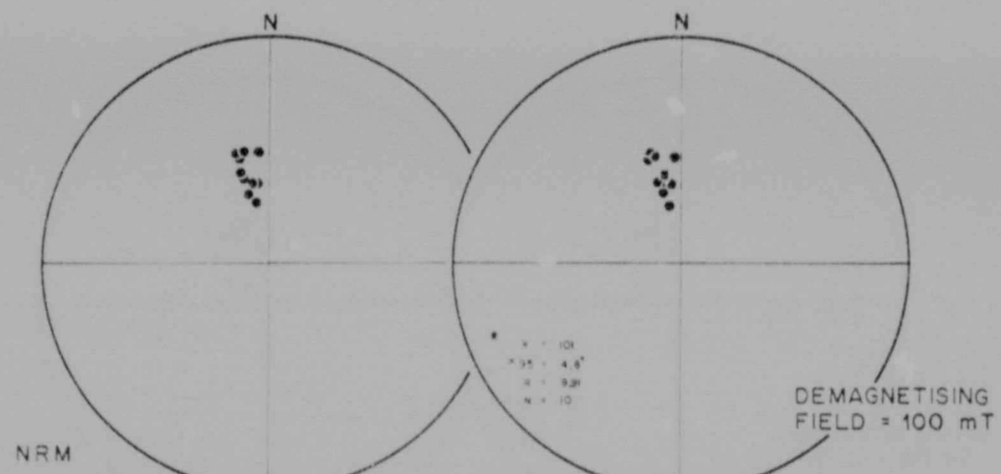

SITE 22 HOLLANDS DOME : ALASKITIC GRANITE

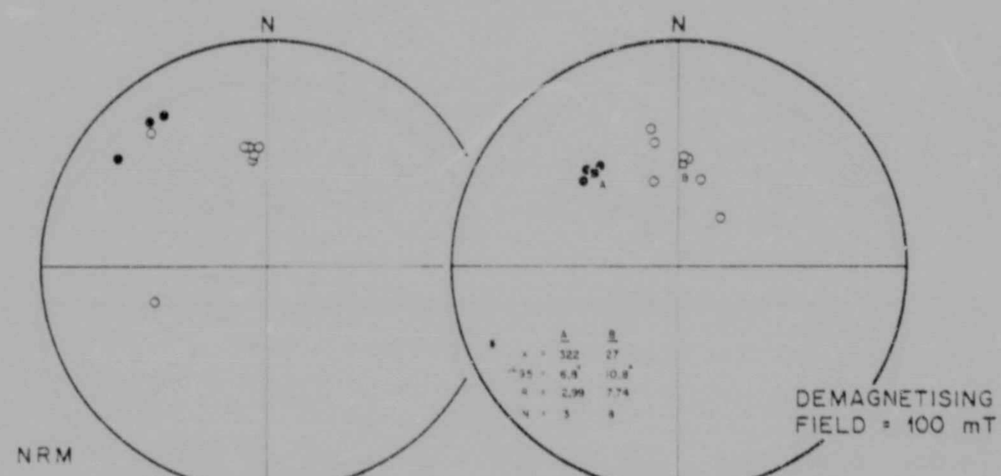

SITE 23 HOLLANDS DOME : KHAN FORMATION

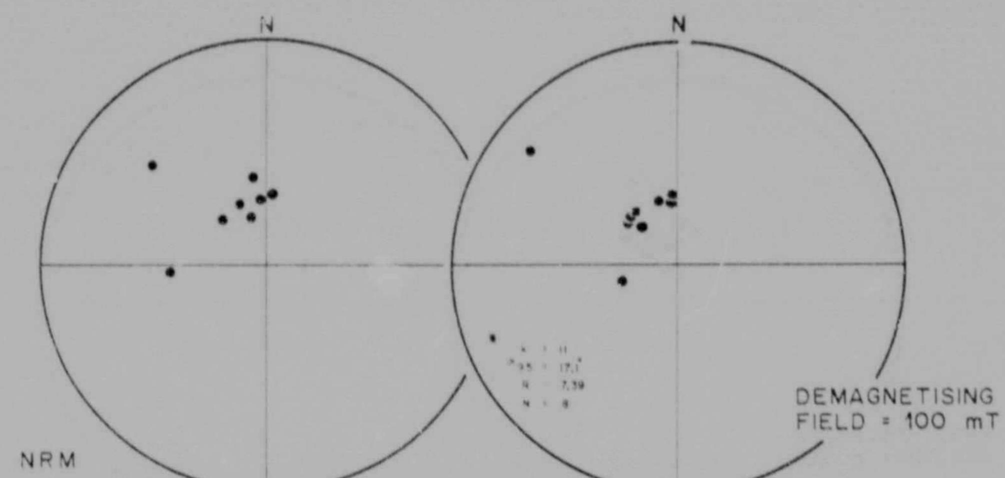

SITE 24 HOLLANDS DOME : ALASKITIC GRANITE

• POSITIVE INCLINATION
○ NEGATIVE INCLINATION

■ □ SITE MEANS
• FISHER STATISTICS AS DEFINED IN TEXT

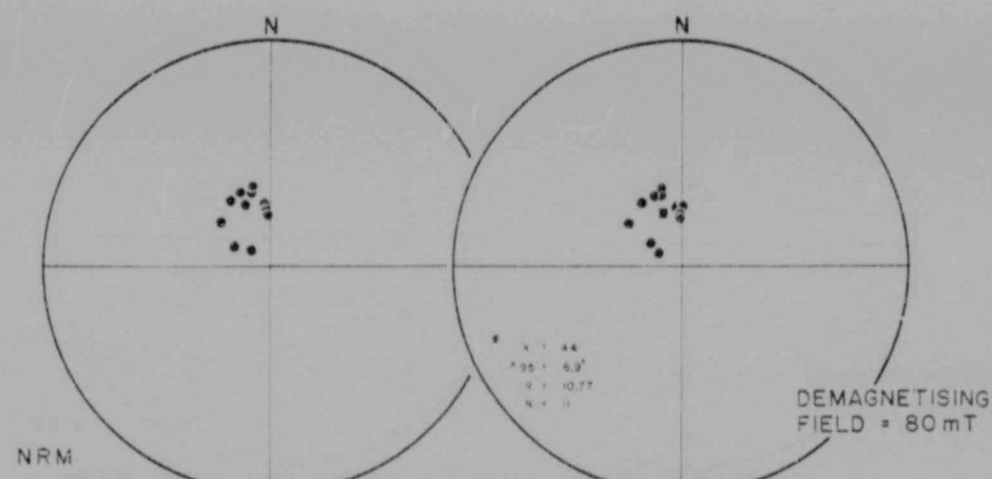

SITE 25 IDA MINE : KHAN FORMATION

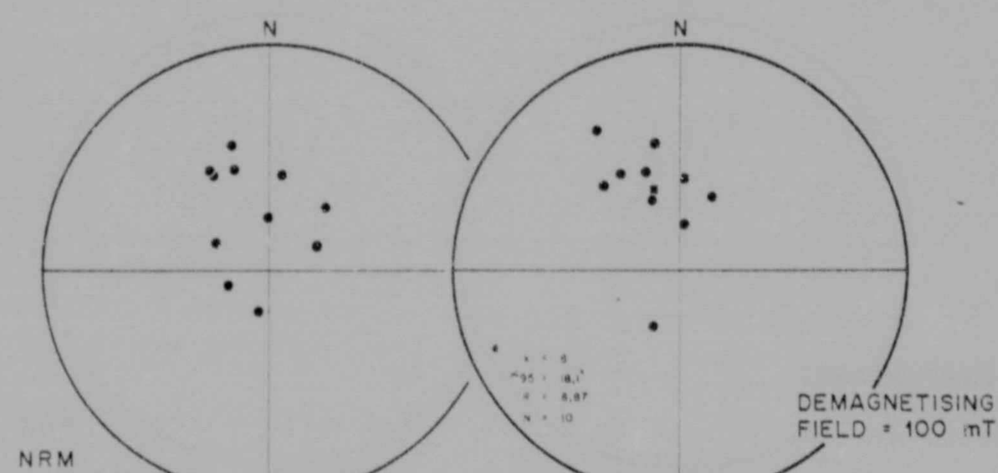

SITE 26 IDA MINE : ALASKITIC GRANITE

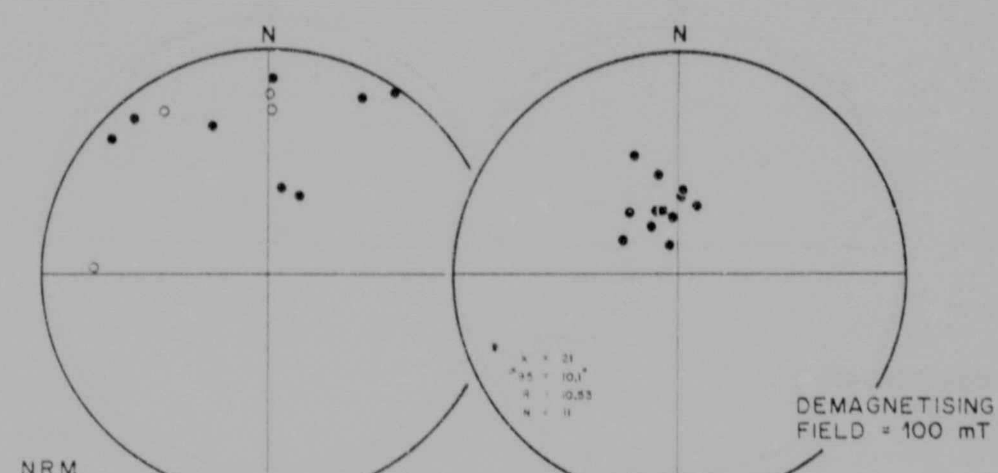

SITE 27 IDA MINE : ALASKITIC GRANITE

● POSITIVE INCLINATION ■ □ SITE MEANS

○ NEGATIVE INCLINATION • FISHER STATISTICS AS DEFINED IN TEXT

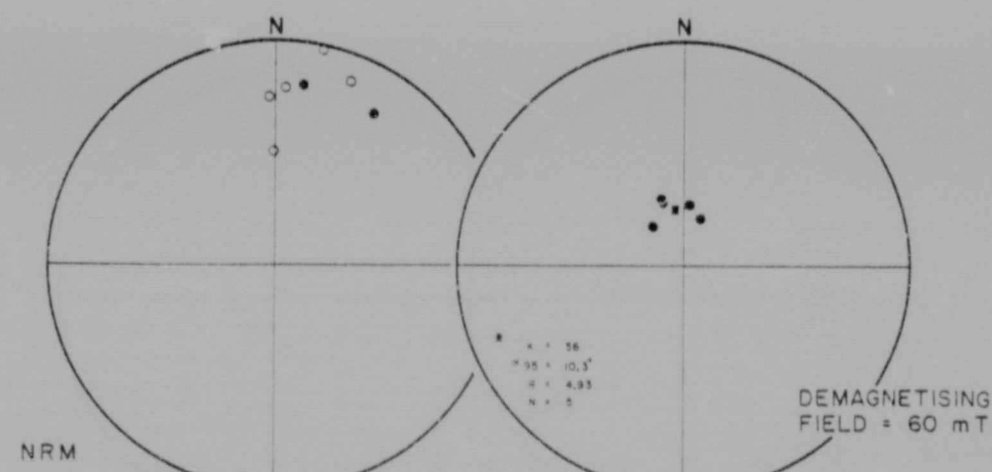

SITE 28 HOLLANDS DOME : RED GRANITE

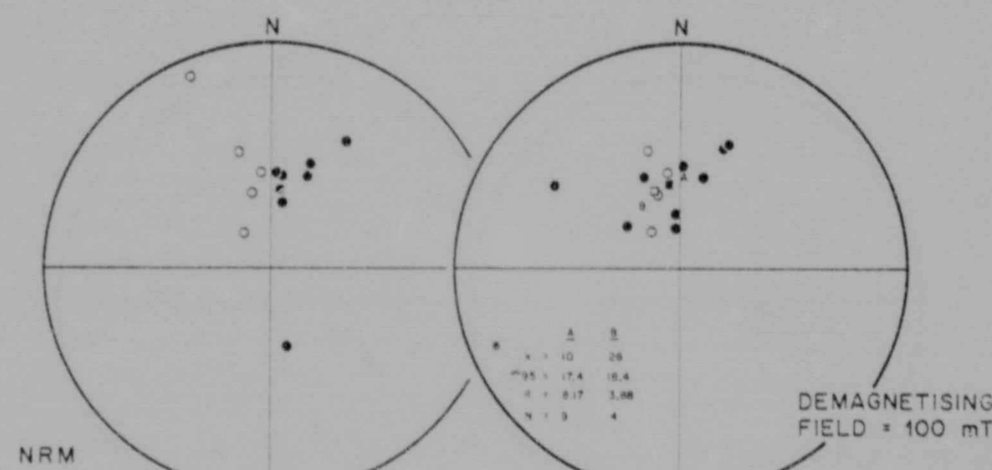

SITE 29 IDA DOME : ALASKITIC GRANITE SHOWING OXIDATION HALOES

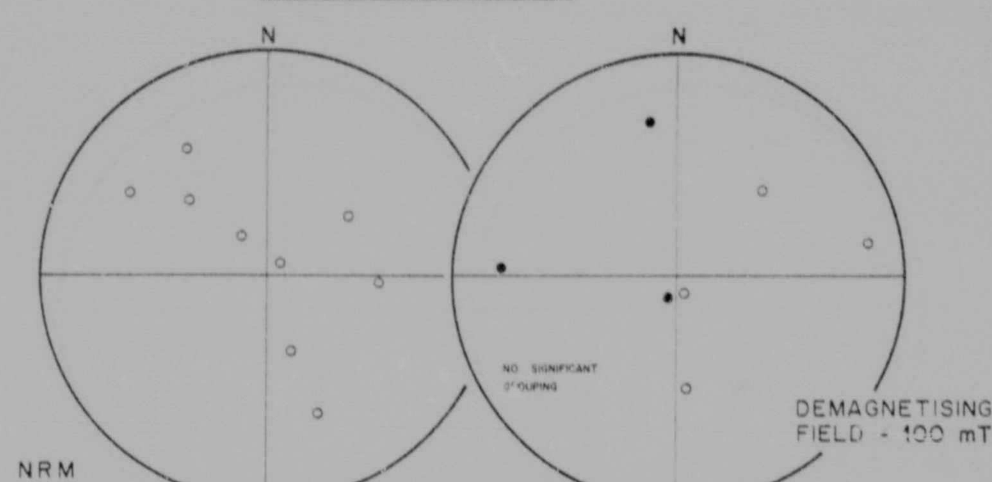

SITE 30 ONANIS : DONKERHUK GRANITE

● POSITIVE INCLINATION
○ NEGATIVE INCLINATION
■ □ SITE MEANS
* FISHER STATISTICS AS DEFINED IN TEXT

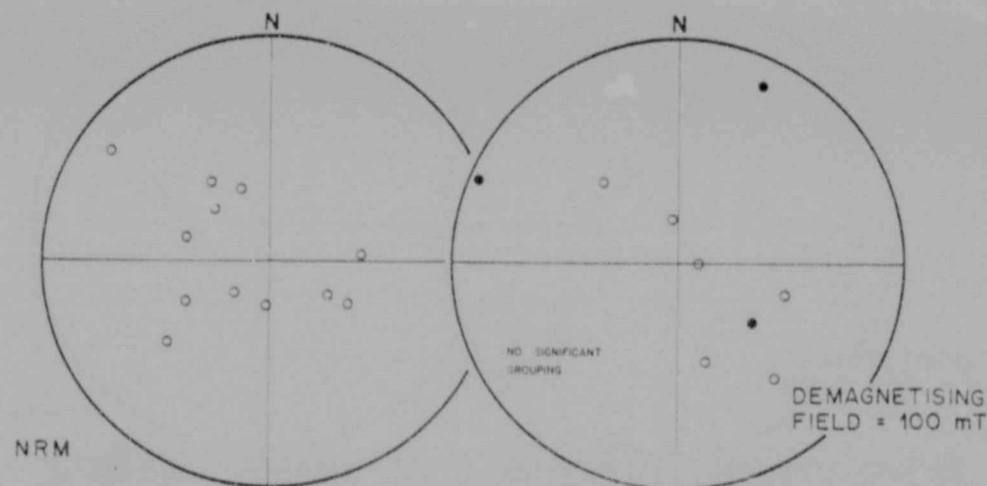

SITE 31 ONANIS : DONKERHUK GRANITE

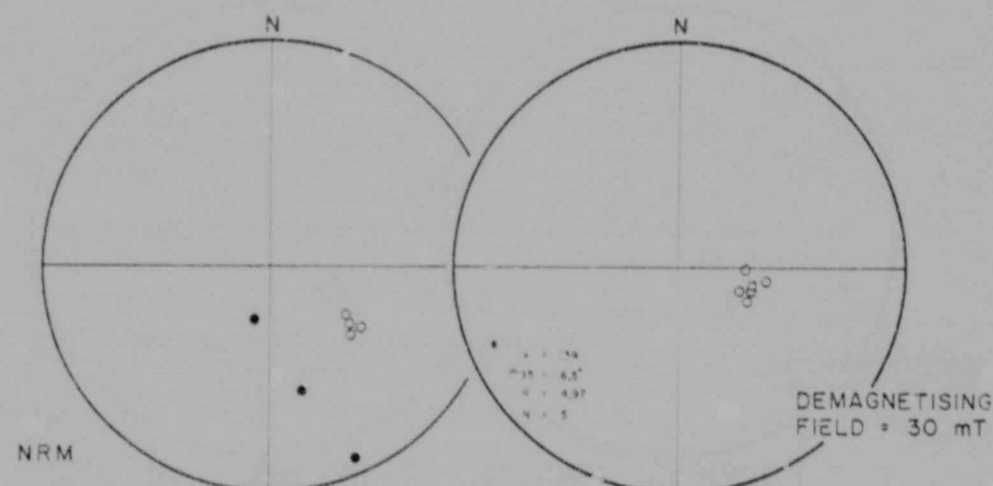

SITE 32 SOLITAIRE - 412 : PIKSTEEL GRANODIORITE

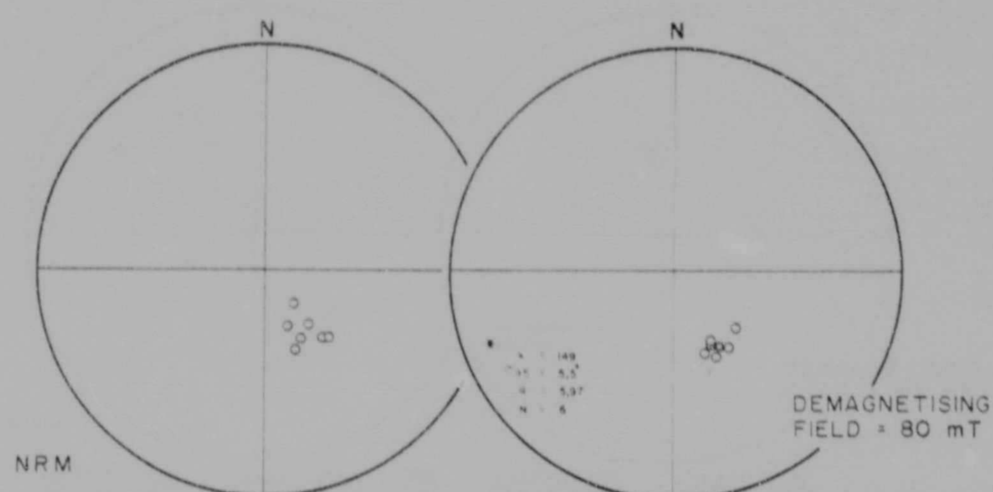

SITE 33 FARM - 399 : PIKSTEEL GRANODIORITE

• POSITIVE INCLINATION ▪ ▫ SITE MEANS

○ NEGATIVE INCLINATION • FISHER STATISTICS AS DEFINED IN TEXT

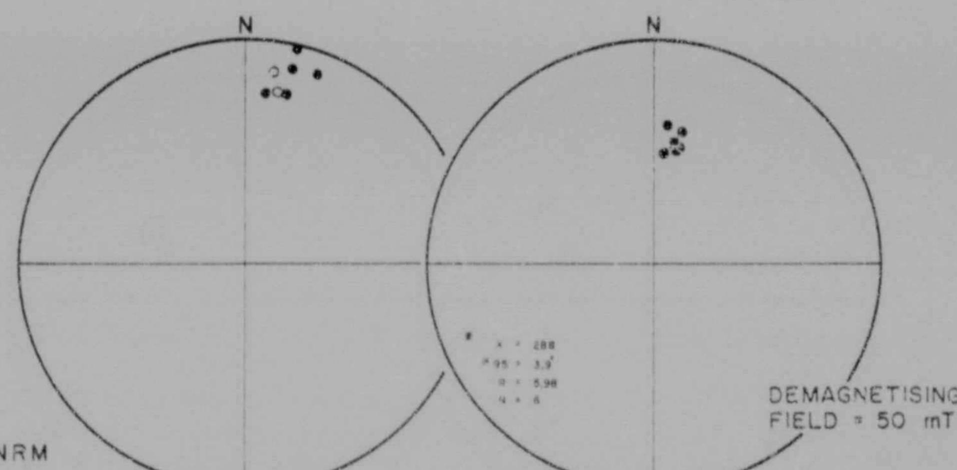

SITE 34 ABBABIS-70 : BASEMENT GRANITE-GNEISS

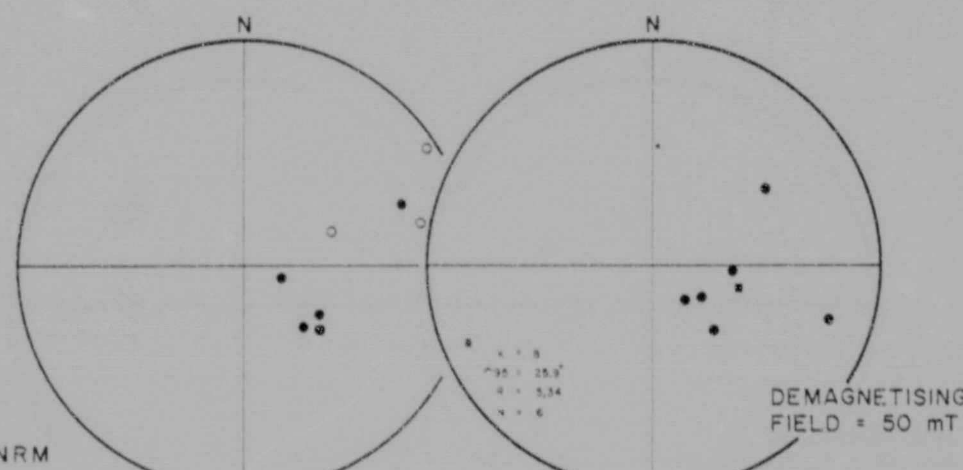

SITE 35 UBIB (W) - 76 : ABBABIS COMPLEX

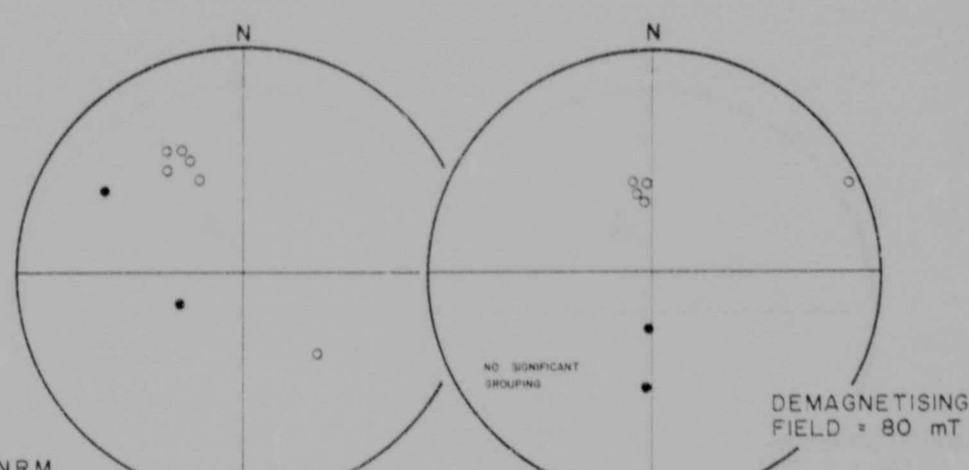

SITE 36 UBIB (W) - 76 : ABBABIS COMPLEX

• POSITIVE INCLINATION
○ NEGATIVE INCLINATION
■,□ SITE MEANS
* FISHER STATISTICS AS DEFINED IN TEXT

SITE 37 CAPE CROSS COMPLEX

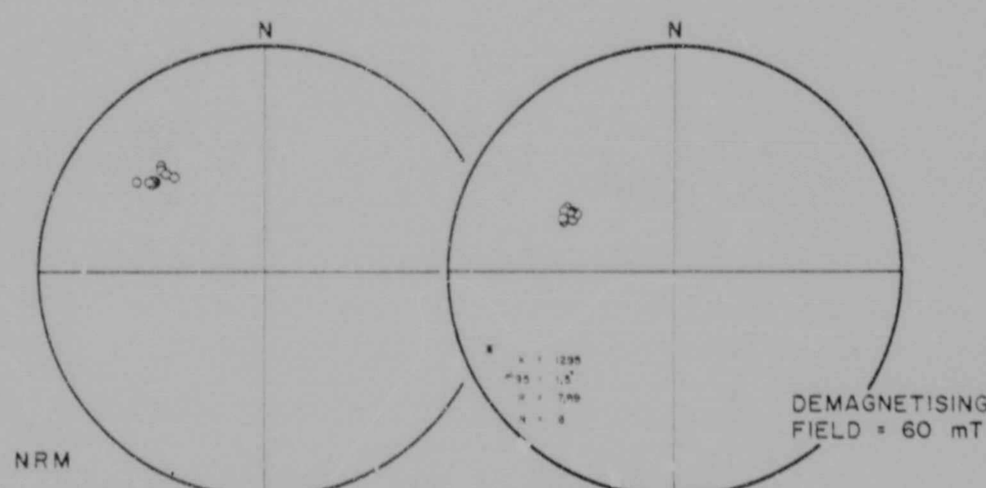

SITE 38 CAPE CROSS COMPLEX

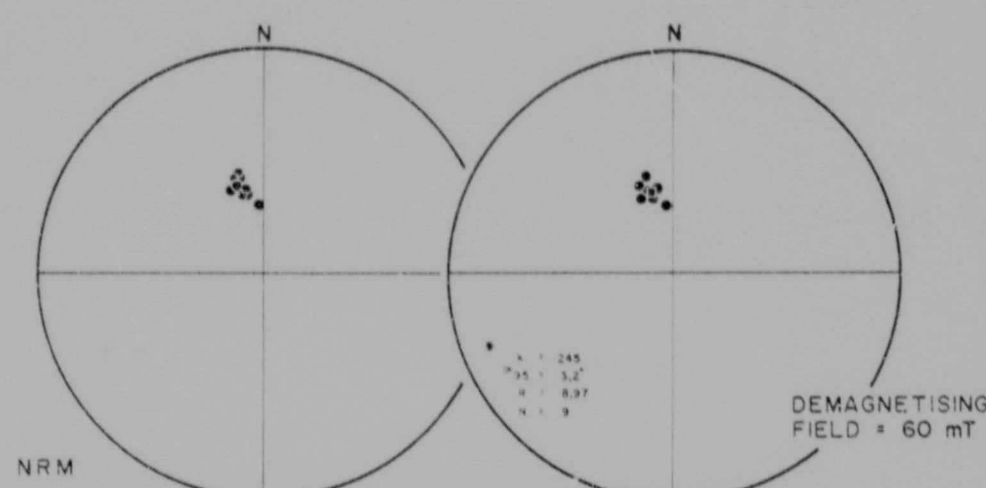

SITE 39 TSAUN BEACON : KHAN FORMATION

• POSITIVE INCLINATION
○ NEGATIVE INCLINATION
•,○ SITE MEANS
* FISHER STATISTICS AS DEFINED IN TEXT

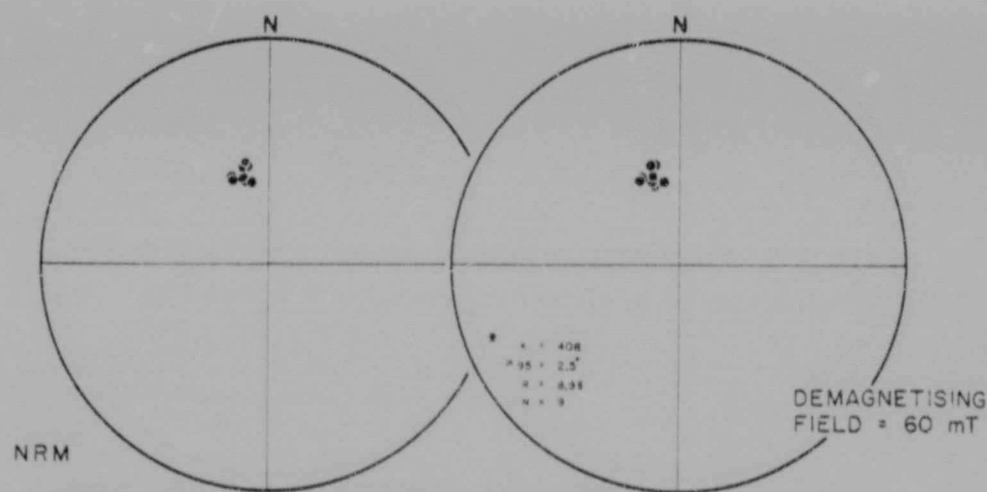

SITE 40 TSAUN BEACON : KHAN FORMATION

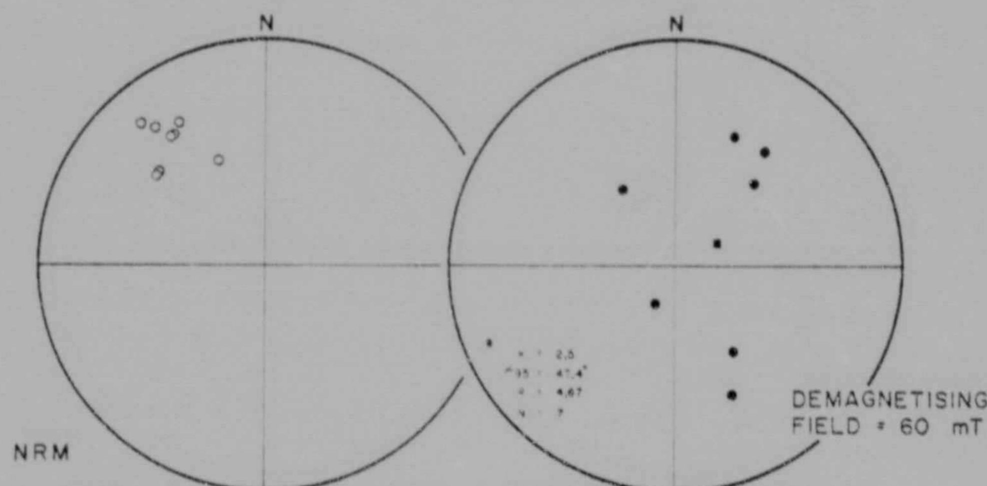

SITE 41 TSAUN BEACON : KHAN FORMATION

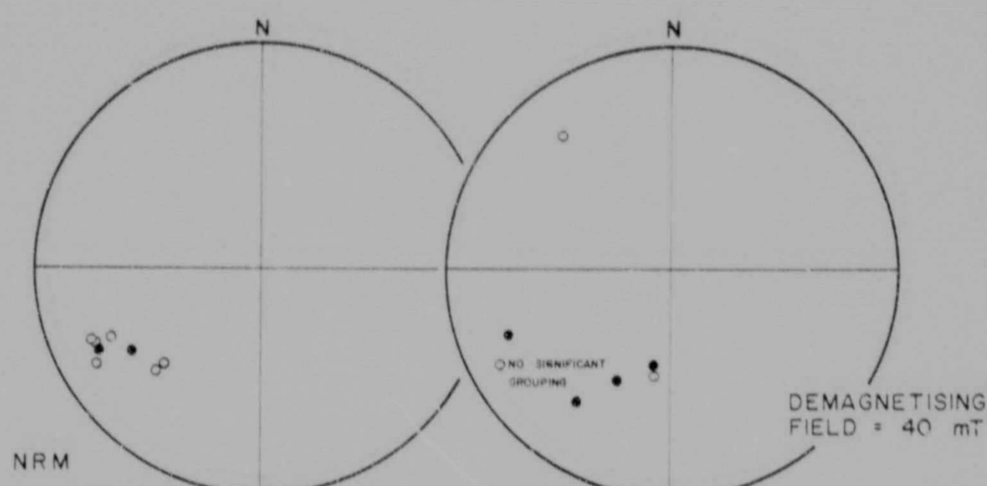

SITE 42 BRANDBERG GRANITE

● POSITIVE INCLINATION ■,○ SITE MEANS

○ NEGATIVE INCLINATION • FISHER STATISTICS AS DEFINED IN TEXT

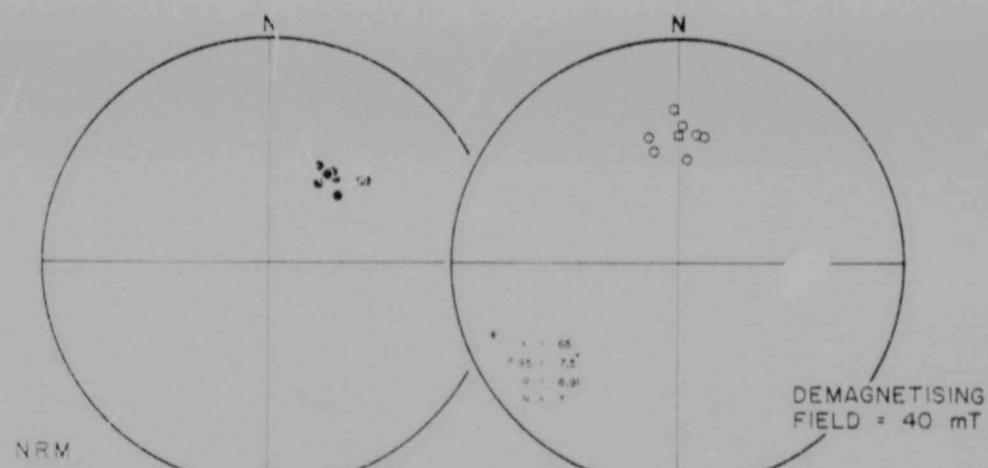

SITE 43 BRANDBERG GRANITE

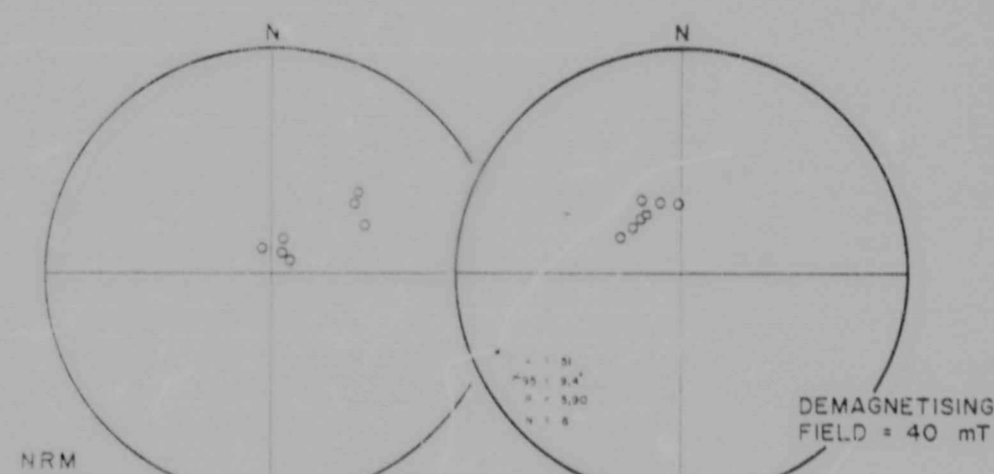

SITE 44 ANIBIB - 136 : ERONGO GRANITE

SITE 45 AMEIL - 60 : ERONGO GRANITE

• POSITIVE INCLINATION ■ □ SITE MEANS

○ NEGATIVE INCLINATION * FISHER STATISTICS AS DEFINED IN TEXT